

Potentiodynamic electrochemical impedance spectroscopy

G.A. Ragoisha*, A.S. Bondarenko

Physico-Chemical Research Institute, Belarusian State University, 220050 Minsk, Belarus

Available online 23 November 2004

Abstract

Potentiodynamic electrochemical impedance spectroscopy (PDEIS) uses virtual instruments to acquire, by means of a common potentiostat, multidimensional dependencies that characterise variations of dc current and frequency response in the same potential scan. Unlike classical EIS, which finds the whole equivalent circuit in stationary states, PDEIS finds, in potentiodynamic systems, only those elements of equivalent circuits that are needed to decompose the ac response in a limited range of frequencies. The decomposition of ac response into components belonging to different elements is provided by a built-in spectrum analyser, which gives dependences of equivalent circuit parameters on variable potential. The new technique develops the idea, originally suggested by D.E. Smith, of versatile characterisation of the electrochemical response in a simple computerised experiment. PDEIS solves this problem with the use of multi-frequency potentiodynamic probing based on analysis of streams of wavelets. The use of the additional variable (electrode potential) helps to disambiguate the equivalent circuit analysis. The PDEIS performance is illustrated on systems of different kind: a reversible system (ferricyanide redox transformations on glassy carbon and platinum electrodes), a system that is locally reversible but shows different responses in forward and backward scans (Bi up on Au) and strongly irreversible variable system (initial stages of aniline electropolymerisation on gold).

© 2004 Elsevier Ltd. All rights reserved.

Keywords: Electrochemical impedance; PDEIS; Underpotential deposition; Bismuth; Electropolymerisation; Polyaniline

1. Introduction

Electrochemical responses contain valuable information both on interfacial structures and dynamics of interfacial processes. The established practice of the electrochemical characterisation implies sequential probing of the electrochemical system with various techniques, highly specialised in particular aspects of ac and dc responses [1,2]. The separate analysis of the frequency and potential variance of the response, as well as the separate investigation of ac and dc responses has been inherited by the present-day computerised techniques from the analog predecessors that were unable to monitor the multidimensional dependences in a single potential scan. The dispersal of the electrochemical response investigation among different techniques is very disadvantageous, especially to the mutable and non-stable systems characterisation, and this is one of the main limitations for a wider application of electrochemical techniques in surface science. Each

of the components of the electrochemical response has a notable potential for interfacial studies: a double electric layer is the thinnest probe, which helps to detect even the slightest changes on the interface by the variation of the double layer capacitance, the Faradaic responses are remarkably sensitive as well as selective, and the responses of electronic processes in semiconductor space charge layers on electrochemical interfaces provide unique possibilities for investigation of tiny semiconductor structures. However, on the whole, the techniques of electrochemistry are often considered in surface science among supplementary techniques [3]. The losses of opportunities originate from the above-mentioned disintegration of the electrochemical probing between different techniques and the difficulties of components separation in complex responses, which hinder the development of practically feasible integrated probing procedures for the comprehensive characterisation of electrochemical systems.

The idea of versatile characterisation of the electrochemical response in a single computerised experiment was first suggested by Smith with co-workers [4–8], who developed the concept of Fourier transform electrochemical instrumen-

* Corresponding author. Fax: +375 17 2264696.

E-mail address: ragoishag@bsu.by (G.A. Ragoisha).

tation, which was elaborated later [9–11] for application on personal computers. Fourier transform electrochemical instrumentation uses simultaneous multi-frequency probing and gives the transfer function by comparing the current signal spectrum with the voltage spectrum [5]. Repetitions of the same procedure on each step of a staircase potential scan give frequency responses as functions of electrode potential. Though the Fourier transform electrochemical instrumentation has been elaborated for three decades, it has not replaced the common ac and dc voltammetry. The main problem with that technique comes from a very low intensity of the constituent responses and their non-uniformity. The simultaneous analysis of multi-frequency responses is much more restricted than the single-frequency analysis. Responses in different frequencies may differ in orders of magnitude; therefore even small nonlinearity of the most intensive component, which might be insignificant in the single-frequency probing, hinders considerably the acquisition of low-level components. The hindrance depends on the properties of the system under investigation and therefore cannot be taken into account before the measurement. For this reason the optimisation of phases, which allows composing the probing signal with the amplitude much lower than the sum of the constituents [11], does not always result in the optimal response. Equivalent electric circuit (EEC) analysis with Fourier transform electrochemical instrumentation is difficult and very few publications (see e.g. [12,13]) are available on the application of that technique for decomposition of the potentiodynamic frequency response into constituents related to EEC elements.

The fundamental alternative to frequency response acquisition with Fourier transform techniques that overcomes intrinsic limitations in accuracy of simultaneous frequency response analysis is the application of wavelets [14,15]. Wavelets are small waves terminated on the time scale. Due to the termination, each frequency can be treated individually in streams composed of many wavelets, and this gives the benefit of better response protection from the effects of nonlinearity and noise. However, frequency scanning with wavelets requires sophisticated real-time virtual instruments capable of precise positioning of the probing and analysis in the streams of responses (in the wavelet approach the frequency response is analysed locally in different parts of the time series, unlike the case with FFT, when the whole signal is analysed simultaneously).

The potentiodynamic electrochemical impedance spectroscopy (PDEIS) [15] uses a common potentiostat and virtual instruments on a personal computer for electrochemical system probing with streams of mutually coordinated wavelets and real-time analysis of the response. Similarly to the Fourier transform electrochemical instrumentation, PDEIS superimposes ac probing on the staircase potential scan for the acquisition of frequency response variation. Due to high power of modern computers and low-level optimisation of virtual instruments, the snapshots of the frequency response can be taken in PDEIS for hundreds or even several

thousand times during the potential scan (the scan may be either unidirectional or cyclic) with real-time representation of the variation of the frequency response and dc current on a computer screen. The EEC analysis in PDEIS is implemented in the virtual spectrometer subroutine that utilises three different minimisation algorithms in order to provide reliable fitting. PDEIS was used for characterisation of Cu upd on gold [16], Pb upd on Te [17] and Ag upd on Pt [18].

In this work PDEIS was applied to systems of various kind: (i) reversible, (ii) locally reversible but irreversible in a wider potential range, and (iii) completely irreversible. In each of the cases PDEIS provided different but substantial opportunity for diversified fast characterisation of objects under investigation. The combination of impedance spectroscopy, which is originally a stationary technique, with the intrinsically non-stationary approach of potentiodynamic techniques, appears to be constructive and helpful, despite some self-contradiction of joining seemingly opposite approaches. The contradiction is actually just seeming, as the impedance itself is not a stationary characteristic but just a relation of the ac voltage to the ac current, which makes sense both for stationary and nonstationary systems. The stationarity in common EIS is required mainly for measurements in infralow frequencies, therefore the latter have to be cut off in potentiodynamic measurements. As a trade-off, the EECs obtained by PDEIS can be incomplete. PDEIS does not attempt to derive a complete EEC for an object under investigation. Unlike common EIS, PDEIS investigates just a part of a transfer function and concentrates on the evolution of the acquired part of frequency response in the potential scan. The situation with EIS and PDEIS is similar to the situation with stationary and potentiodynamic, in particular cyclic, voltammetry. Both the voltammeteries have different applications, and only in certain cases they can be interchangeable. The main destination of PDEIS is the characterisation of variable interfaces. This aspect of PDEIS was considered recently [17] on the example of irreversible Pb upd on Te, the system complicated by a spontaneous interaction of Pb monolayer with the substrate. By applying PDEIS in this work to systems of various kinds, we tried to present a wider view of the possibilities of the versatile potentiodynamic response characterisation in the systems with different extent of irreversibility.

2. Experimental

PDEIS spectra were recorded using a technique that was described in [15]. PDEIS virtual spectrometer is a computer program that acquires ac and dc responses by means of a common potentiostat. The control of the PDEIS spectra recording is very similar to the control of CV acquisition in common computerised potentiostats. The potential and frequency ranges, periodicity of frequency response snapshots, scan rate, number of cycles of the potential scan, ac amplitude and several other parameters were set from the interface of PDEIS 1.4 program before the scan. Ac amplitude of the

probing signal was from 5 to 10 mV and the potential steps in the potential scan were always set to be several times smaller than the ac amplitude. This secured the continuity of spectra. Similarly to CV, PDEIS requires continuity of the recording to give accurate representation of the dynamics of the response variation on the potential scale.

Using very small potential steps was also important for data clearance from random noise and compensation of drift effects, which could be generated by the potential scanning. Interpolation in sequences of repeatedly acquired impedance spectra is a usual way of drift compensation in nonstationary impedance measurements [19]. PDEIS utilises this possibility in the smoothing of 3D data along the potential scale before EEC fitting of the data in constant potential sections. Distances on the potential scale between neighbouring 2D sections of 3D PDEIS spectrum are smaller than the ac amplitude. This enables addition of information from several neighbouring sections to each 2D section by applying a moving average smoothing in the range commensurable with the ac amplitude, which results in more reliable fitting in the constant potential sections of the spectrum.

It is well known [20] that the accuracy of impedance data is very dependent on the frequency. Common nonlinear least squares fitting spreads the errors from the least accurate part of the spectrum over the whole spectrum, however local fitting for the most accurate part of the spectrum gives much better result for that part of the spectrum. PDEIS benefits from this possibility by using relatively narrow fractions of EIS spectra in the ranges of the maximal accuracy of the equipment. In the examples that will be considered in this work the spectra were previewed in the range from 5 Hz to 3 kHz and recorded for quantitative analysis in the following ranges:

- (i) $[\text{Fe}(\text{CN})_6]^{3-}$ reduction on glassy carbon: from 20 to 351 Hz;
- (ii) $[\text{Fe}(\text{CN})_6]^{3-}$ reduction on Pt: from 14 to 1750 Hz;
- (iii) Bi upd on Au: from 27 to 877 Hz;
- (iv) aniline electropolymerisation on Au: from 12 to 433 Hz.

We would like to emphasise that the EEC fitting in such narrow ranges purposes the decomposition of the actual *acquired* response, and PDEIS does not attempt to derive a complete EEC, which might probably require much wider spectra. Even in ac voltammetry, which acquires a single frequency response, the response originates from different EEC elements, but the ac voltammetry has no means to decompose its responses, because the decomposition requires the knowledge of the frequency response. Fortunately, only a part of the transfer function is needed to decompose the ac response at a certain frequency, and this makes the basis for the potentiodynamic frequency response analysis. Thus, PDEIS solves a quite different problem than the stationary EIS does – this new technique investigates the evolution in the potential scan of those EEC elements whose responses fall into the analyser window. The narrow frequency range used in PDEIS may seem unusual from the point of view

of the stationary impedance spectroscopy but actually most spectroscopic techniques deal with small frequency ranges, as well as kinetic studies are often limited in certain ranges of time constants.

PDEIS can analyse short-cut spectra not only due to the above mentioned optimisations but also, and mainly, due to the additional variable, the potential that helps to check the consistency of the fitting which could be otherwise very ambiguous.

Actually, PDEIS solves the problem in three dimensions, unlike stationary EIS, which operates on 2D data. We have implemented two strategies of finding the EEC with the built-in fitting routine. The first one is used for the systems that have no theoretically predicted models. This strategy utilises the automatic enumeration of possibilities on several constant potential sections of the 3D spectrum from more than 20 circuits (most often used in EIS analysis) with the automatic rating, which reduces the number to very few circuits for a subsequent more detailed analysis of the behaviour on the potential scale. This strategy has been used in the investigation of the initial stages of polyaniline film growth in aniline electropolymerisation (Section 5), as there was no presupposed model for the nonstationary ac response of that system. The other strategy proceeds from theoretical assumptions that give fewer models for trying. Thus, the Randles circuit was tried as the first approximation for simple reversible reactions considered in Section 3, and models of reversible adsorption gave the possible variants for the EEC of Bi upd. The next paragraph explains the strategy of deriving the EEC of Bi upd on gold.

A linear component of the ac electrochemical response of an upd at a small perturbation of the electrode potential ΔE may be presented in the following functional form [21,22]:

$$\Delta i = \left(\frac{\partial i}{\partial E} \right) \Delta E + \left(\frac{\partial i}{\partial \theta} \right) \Delta \theta + \left(\frac{\partial i}{\partial C_s} \right) \Delta C_s \quad (1)$$

where Δi , ΔC_s , $\Delta \theta$ are the respective variations of the current, metal cation surface concentration and surface coverage of metal adatoms formed as a result of upd. In the case of reversible upd the first term produces a resistance, the second – the adsorption capacitance, and the third – the impedance of diffusion. In the upd with anion coadsorption, depending on the mechanisms, the adsorption of cations and anions may appear in frequency response either as a single process, or as two separate processes. Assuming additivity of the both adsorption processes and the double layer charging [23], one obtains two RCW branches in parallel with the double layer capacitance [12,13], where R is the resistance, C the adsorption capacitance and W is the Warburg element in the EEC. Inseparable adsorption of cations and anions would produce just one RCW branch for the Faradaic part of impedance. In all cases a serial resistance should be added to account for the damping effect of solution. Also, reduced versions, lacking some of the above-mentioned components of the Faraday impedance, should be tried, to take account of the shortcut-

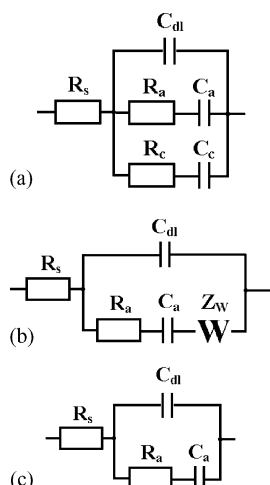


Fig. 1. Equivalent circuits for Bi upd on Au that were selected at preliminary examination of spectra.

ting of the spectra. Not all of the three components of Faraday impedance are equally pronounced in different upd processes. In a reversible upd the out-of-phase component of the Faraday impedance is predominantly capacitive [24,25], while in the irreversible upd it turns to be completely diffusional [17]. In the latter case adsorption capacitance vanishes, because the oscillation of the adatom coverage, which produces this EEC element, requires the overlap of the potential ranges of the upd and the monolayer desorption. In Pb upd on Te [17] and Ag upd on Pt [18] the cathodic and anodic processes did not overlap and therefore no capacitance of adsorption showed up in the EEC. On the contrary, Bi upd on Au has been found in this work to behave typically capacitive, due to overlap of cathodic and anodic processes.

Fig. 1 shows a subset of the three circuits that remained after preliminary rating of the EECs from the above-mentioned wider set, and Fig. 2 gives two examples of Nyquist plots with the best fit lines for the three models. The circuit (c) showed insufficient fit and thus was easily excluded, but the circuits (a) and (b) both fitted to the data with χ^2 less than 10^{-4} in the constant potential sections shown in Fig. 2. In terms of a single spectrum analysis this two models seem to be indis-

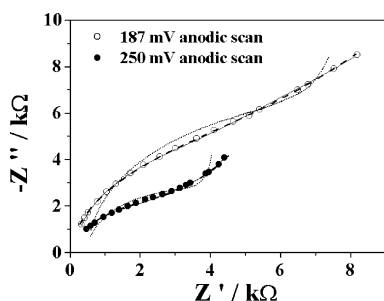


Fig. 2. Examples of Nyquist plots for two constant potential sections of PDEIS spectrum of Bi upd on Au in perchloric medium with the best fit lines corresponding to different circuits from Fig. 1: (a) solid, (b) dashed, and (c) dotted.

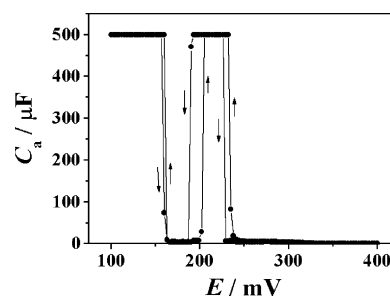


Fig. 3. Illustration of impedance data unstable fitting with the model shown in Fig. 1b (C_a variation in the cyclic potential scan).

tinguishable in certain 2D sections of the PDEIS spectrum. However, with the variable potential the minimisation procedure for the model (b) appeared to be unstable (Fig. 3, the higher value of C_a is the upper limit of the minimisation procedure which was excessively assigned to be of 500 μF). The abrupt transitions of C_a were physically unlikely with the potential changes smaller than the amplitude of ac perturbation and also accuracy of fit (χ^2 and relative errors for individual elements) in general was not sufficient to accept model (b) even for limited ranges of the potential. On the contrary, model (a) gave reasonable potential dependences of the EEC elements with χ^2 far below 10^{-4} and low relative errors for individual elements. The dependences of the EEC elements for this model will be considered in Section 4.

Thus, the EEC fitting can be ambiguous in single short-cut spectra, but the knowledge of the variation of the frequency response with the potential helps to resolve the ambiguity. Due to variation of contributions of different processes to the total response, it is hardly possible to obtain smooth fitting in three dimensions for incorrect model, though the ambiguity of single spectra is a common problem in EIS.

Because of the variable potential, the EEC fitting in PDEIS differences from the fitting in common EIS also in the amount of calculations. The processing of thousands of spectra was difficult with common CNLS programs, as the stability of the fitting procedures turned to be very important in the automated processing. This made us to implement a coherent processing of large sets of the 2D sections of the 3D PDEIS spectrum in the spectrometer built-in fitting routine. Upon trying manually various reasonable models at several potentials or rating them automatically, the fitting to the prospective model runs automatically along the potential scale in such a way that the solution obtained in one section is used as the first approximation for the minimisation in the next section. The resulting coherency of the analysis, together with the use of three minimisation algorithms [15] and permanent control of χ^2 and relative errors of EEC elements, provided stability and reasonable reliability of the automatic fitting. Good models keep χ^2 below 10^{-4} in the whole range of the potential, while sharp changes in χ^2 and in relative errors for individual elements disclose either incorrectness of the model, or inappropriateness of presumed limits for the parameters (presumptions on possible limits for parameters

variation based on their physical reasonability help to make the automatic minimisation more stable than the minimisation in unbounded ranges).

In order to enable reliable signal processing around 50 Hz, where noise of a power supply could make a problem, we used an updated 1.4 version of the spectrometer program [18] with digital elimination of the 50 Hz noise from the responses in neighbouring frequencies. The digital noise elimination was based on superposition of signals with different phase shifts.

The PDEIS spectrometer can record and analyse continuously thousands of 2D impedance spectra in multi-cyclic scans. However, simultaneous recording of several cycles was inconvenient from the point of view of visual data presentation, therefore normally we stopped the scan in the end of each cycle to save the data to disc and started a new recording for the next cycle. The dynamic impedance spectra were plotted on a computer screen just in the potential scan, but the analysis of the spectra with the built-in EEC fitting routine was implemented after the scan. The cyclic PDEIS spectrum is represented on the screen by two surfaces – the variable potential extensions of common 2D impedance spectra in the coordinates of either Nyquist, or Bode plots. One of the surfaces corresponds to the forward scan and the other – to the backward scan. The voltammograms and impedance spectra were software extracted from the same complex response.

Coincidence of the two surfaces that characterise forward and backward scan is an obvious indication of high reversibility of the system (this case will be considered in Section 3), while a mismatch of the two surfaces discloses the irreversibility, which is sometimes not obvious in cyclic voltammograms [16]. That peculiarity was considered on the example of Cu upd on Au [16], and in this work we consider a more complex reversible upd system (Bi upd on Au) that also manifests considerable irreversibility in the reverse scan. Bi upd on Au, similarly to Cu upd on Au, is reversible in the sense of existence of characteristic adatom coverage at each potential, which produces the capacitance of adsorption. However, because of formation of complex adsorption structures with the participation of anions, the creation of the monolayer in the cathodic scan and its destruction in the anodic scan goes by different paths. PDEIS, as a nonstationary technique, appears to be capable to give much information to characterise this difference.

PDEIS spectroscopy is an entirely virtual technique. It implements all the functions with computer program that interacts with the object by means of a potentiostat. In this work we used an inexpensive PI-50 potentiostat as the only hardware besides the computer and its ADC/DAC interface. In order to make sure that the probing and analysis algorithms work reliably and produce correct information about objects under investigation, two kinds of control have been used – the operation control on sample electric circuits [26] and the control of compliance to the theoretically predicted behaviour on the reversible systems whose potentiodynamic frequency response is generally predictable. One of the goals of investigating a simple reversible system (Section 3) with

PDEIS was the comparison of the behaviour of the technique with theoretical expectations for ac response of a reversible system.

The experiments were performed in a conventional three-electrode electrochemical cell using Ag|AgCl|KCl(sat.) reference electrode. To prevent the contamination of the working solutions by chloride, the reference electrode was placed in a tap-isolated compartment of the electrochemical cell. A platinised Pt counter electrode of high surface area was used to eliminate the counter electrode impedance from the total measured impedance.

Working electrodes of three different kinds were used in this work. Glassy carbon and platinum electrodes (0.07 and 0.008 cm² surface area, respectively) were used in experiments with a reversible [Fe(CN)₆]³⁻/[Fe(CN)₆]⁴⁻ system. Polycrystalline gold wire (ChemPur) was used for Bi upd and aniline electropolymerisation. Au-electrode surface area was 0.03 cm².

Aqueous 5.2 mM K₃[Fe(CN)₆] + 1 M KCl solution was used for reversible reaction examination. To investigate the effect of 1-thioglycerol adsorption on charge transfer, Pt electrode was immersed into 0.5 mM aqueous solution of 1-thioglycerol for 20 min and afterwards rinsed with distilled water.

Gold electrode was flame annealed in each experiment before Bi upd and after cooling in air placed into one of the following electrolytes: (1) 5 mM Bi(NO₃)₃ + 0.3 M HNO₃ and (2) 5 mM Bi(ClO₄)₃ + 0.3 M HClO₄.

Polyaniline film was grown by cyclic potential scanning of Au electrode between 800 and –100 mV in aqueous 80 mM C₆H₅NH₂ + 1 M HCl solution. All working solutions used in this work were deaerated with nitrogen for 20 min before each experiment.

3. Reversible reaction

PDEIS is intended for use mainly with nonstationary mutable systems, where it shows unique information on constituent ac responses dependences on the potential. The investigation of reversible systems was interesting, first of all, for testing the technique itself, as the theory of potentiodynamic ac response is relatively simple in reversible systems and this gives the possibility of comparing the experiment and the theory.

Fig. 4 shows a typical PDEIS spectrum of a reversible [Fe(CN)₆]³⁻/[Fe(CN)₆]⁴⁻ system on a glassy carbon electrode, Fig. 5 shows the best fit equivalent circuit, and Fig. 6 – the variation of the inverse Warburg constant, A⁻¹ in cyclic potential scans with different scan rates. Because of the reversibility of the redox transformations, the negative and positive scans give almost the same spectra and almost the same A(E) dependences both for the different directions of the scan and different scan rates (in the [electronic version](#) the negative scan is shown in red and the positive in blue). Fig. 6 shows also the simulated curve for A(E) dependence resulting from

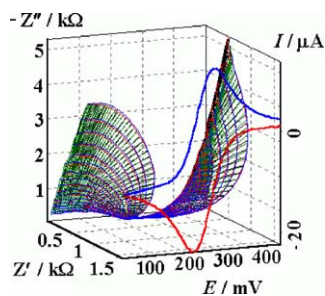


Fig. 4. Cyclic PDEIS spectrum of $[\text{Fe}(\text{CN})_6]^{3-}/[\text{Fe}(\text{CN})_6]^{4-}$ system on a glassy carbon electrode. Electrolyte: 5.2 mM $\text{K}_3[\text{Fe}(\text{CN})_6]$ + 1 M KCl, $dE/dt = 4 \text{ mV/s}$. The CV shown on the transparent front facet of the parallelepiped and the impedance spectrum belong to the same potential scan (the voltammogram and the 3D impedance spectrum were software extracted from the same complex response). The animation is available in the supplement to [electronic version](#).

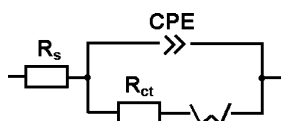


Fig. 5. The best fit EEC to the data shown in Fig. 4. The exponent in the impedance of constant phase element CPE was close to unity.

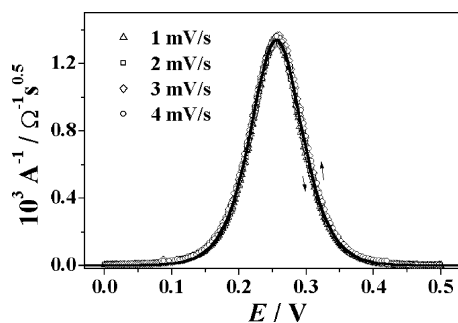


Fig. 6. Inverse Warburg constant variation in cyclic potential scans at different scan rates; experimental data (open symbols) and simulated curve (solid line). Electrode: glassy carbon, electrolyte: 5.2 mM $\text{K}_3[\text{Fe}(\text{CN})_6]$ + 1 M KCl.

the diffusion model which assumes that the initial concentration of the product in the electrochemical reaction is equal to zero. The equations for Warburg constant and charge transfer resistance variation with the potential at this initial condition

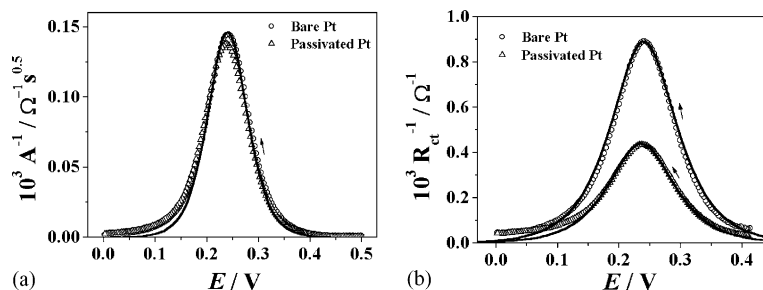


Fig. 7. The effect of 1-thioglycerol adsorption on Pt electrode on inverses of (a) Warburg constant and (b) charge transfer resistance in the cathodic reduction of $[\text{Fe}(\text{CN})_6]^{3-}$. Electrolyte: 5.2 mM $\text{K}_3[\text{Fe}(\text{CN})_6]$ + 1 M KCl, $dE/dt = 1.8 \text{ mV/s}$. Solid lines were obtained by fitting experimental data to Eqs. (2) and (3).

were presented by Lasia in [21]:

$$A(E) = \frac{4RT}{n^2 F^2 A \sqrt{2D_{\text{ox}}c_{\text{ox}}}} \cosh^2 \left[\frac{nF}{2RT} (E - E_{1/2}) \right] \quad (2)$$

$$R_{\text{ct}}(E) = \frac{RT}{n^2 F^2 A \cdot k_0 c_{\text{ox}}} \frac{1 + \exp[nF(E - E_{1/2})/RT]}{\exp[(1 - \alpha)nF(E - E_{1/2})/RT]} \quad (3)$$

where $A(E)$ is Warburg constant, $R_{\text{ct}}(E)$ the charge transfer resistance, D_{ox} the diffusion coefficient of oxidised species, c_{ox} the bulk concentration of oxidised species, F the Faraday constant, R the gas constant, T the absolute temperature, α the transfer coefficient, n the stoichiometric coefficient for number of electrons transferred in the reaction, E the electrode potential, $E_{1/2}$ the reversible half-wave potential, k_0 the standard rate constant, and A is the surface area of the electrode. Diffusion coefficients of reduced and oxidised species were assumed to be equal.

$A(E)$ does not contain parameters of the electrochemical kinetics, while the charge transfer resistance is inversely proportional to the standard rate constant. The consequence of this difference is the capacity of $A(E)$ and $R_{\text{ct}}(E)$ to disclose different aspects of the electrochemical system behaviour. Fig. 7a and b shows this in the thioglycerol adsorption effect on platinum by $A^{-1}(E)$ and $R_{\text{ct}}^{-1}(E)$ dependences in $[\text{Fe}(\text{CN})_6]^{3-}$ cathodic reduction. Thioglycerol adsorption has a weak effect on $A^{-1}(E)$, but $R_{\text{ct}}^{-1}(E)$ is considerably depressed, because of the hindrance to electron transfer resulting from Pt surface passivation by thioglycerol.

Thus, even in simple reversible system, PDEIS may be very useful for fast separation of different constituents of the electrochemical response. The next two sections will show the advantages of mutable systems characterisation with PDEIS.

4. Potentiodynamic frequency responses of bismuth underpotential deposition on gold

Similarly to Cu upd on Au [16,27–29], Bi upd on Au is a reversible process notable for coadsorption of anions [13].

Bismuth upd in perchloric acid, at very low concentration of Bi^{3+} (0.1 mM $\text{Bi}(\text{ClO}_4)_3$ in 0.1 M HClO_4), was investi-

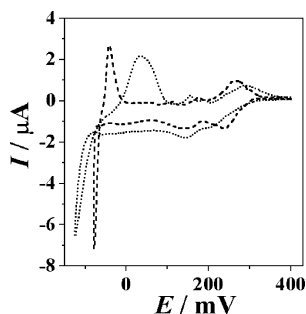


Fig. 8. Cyclic voltammograms of Au electrode in 5 mM $\text{Bi}(\text{NO}_3)_3 + 0.3 \text{ M HNO}_3$ (dashed) and 5 mM $\text{Bi}(\text{ClO}_4)_3 + 0.3 \text{ M HClO}_4$ (dotted). $dE/dt = 66 \text{ mV/s}$.

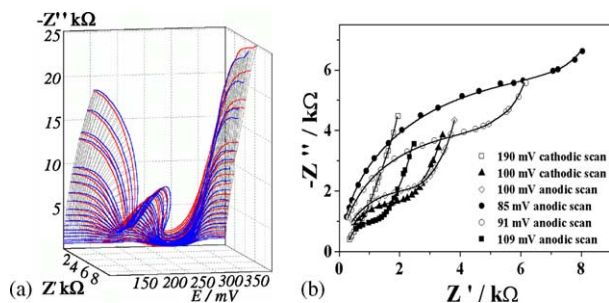


Fig. 9. (a) Cyclic PDEIS spectrum of Bi upd on Au in 5 mM $\text{Bi}(\text{ClO}_4)_3 + 0.3 \text{ M HClO}_4$, (b) constant potential sections of cyclic PDEIS spectrum of Bi upd on Au in 5 mM $\text{Bi}(\text{NO}_3)_3 + 0.3 \text{ M HNO}_3$ (solid lines show fit to the EEC presented in Fig. 1a).

gated with Fourier transform EIS by Garland et al. [13]. In the experimental conditions of [13] frequency responses for nine different potentials from 0.5 to -0.3 V versus SCE were analysed in terms of EEC. Bi upd was found to give just Warburg impedance, while perchlorate produced a separate branch in the EEC, which was assigned to anion coadsorption. The double layer capacitance was found to be almost constant for the whole potential range. The capacitance of perchlorate adsorption showed an increasing trend with the decrease in the potential, which was explained by a stronger affinity for the adsorption at Bi sites than on the bare Au sites.

In this work higher concentrations of Bi^{3+} and anions (5 mM bismuth perchlorate and nitrate in 0.3 M corresponding acid) were used to enhance the capacitive behaviour of the upd, and the potentiodynamic frequency response was acquired continuously in cyclic scans.

Fig. 8 shows cyclic voltammograms of Bi upd and overpotential deposition in perchloric and nitric solutions. Bulk deposition in both solutions proceeds at much lower potentials than the upd and the latter can be easily separated from bulk deposition on the potential scale. In the following frequency response characterisation just the upd range is considered.

Fig. 9a shows the cyclic PDEIS spectrum for Bi upd on Au in perchloric medium (red colour in the [electronic version](#) of the figure corresponds to the cathodic scan and blue colour to the anodic scan), and Fig. 9b – few constant potential sections

of the similar PDEIS spectrum of Bi upd on Au in nitric acid. In both cases reproducible differences of ac responses were observed in forward and backward scans.

The spectra were analysed as described in Section 2 and the analysis gave the equivalent circuit with two separate adsorption processes (Fig. 1a) represented by capacitances and resistances. The dependences of the EEC parameters on the potential for cyclic scans in perchloric and nitric media are shown in Fig. 10.

Fig. 10 contains much information on the dynamics of the constituent processes in Bi upd in different media. The adsorption branch with much higher values of capacitance (its parameters are marked with subscript c) obviously belongs to the cation adsorption (with the opposite assumption the cathodic scan would give positive rather than negative current). Though the signatures of the processes shown in Fig. 10 were well reproducible, we were cautious with interpretation of fine details in this figure, as the accuracy of the separation of two adsorption processes cannot be characterised quantitatively at the present stage of the PDEIS development. However, few general conclusions can be already drawn from these results. First, the effect of anions in the upd is very strong and increases in the cathodic scan. This is evident from the dependences of all parameters on the potential. Second, the effects of irreversibility are non-uniformly distributed on the potential scale and also depend strongly on the anion. The effects of perchlorate begin earlier and fade earlier in the cathodic scan, while nitrate shows its most characteristic signatures between 150 and 100 mV. Third, anions affect considerably the double layer capacitance. The double layer capacitance is much higher and shows more complex changes for nitrate, than for perchlorate, which is probably due to a well-known relative inertness of perchlorate in adsorption processes. However, perchlorate causes a strong hysteresis in the variation of C_{dl} in the cyclic scan. The variation in C_{dl} in perchloric medium was observed in a narrow range of the potential and this effect could be easily overlooked in experiments with few experimental points on the potential scale described in [13]. Adsorption capacitances in the EEC are connected in series with sufficiently large (few $\text{k}\Omega$) resistances, therefore the mixing of the adsorption capacitance with the double layer capacitance in the EEC fitting was hardly possible. In our opinion the variations of the C_{dl} are due to the restructuring of the double layer that takes place because of the monolayer formation and destruction.

The plot of C_a variation with the potential in perchloric medium is notable for its regular character. Using the approach described earlier for sulphate and nitrate adsorption in Cu upd on Au [16], we tested the C_a variation for compliance with Langmuir adsorption model. Fig. 11 shows both the experimental data obtained from the PDEIS spectrum and the simulated curve. In the simulation we used the maximum in $C_a(E)$ as the potential of half-coverage. The experimental data fit well to Langmuir model, but the curve for the reverse scan is shifted to higher potential. This effect also shows that

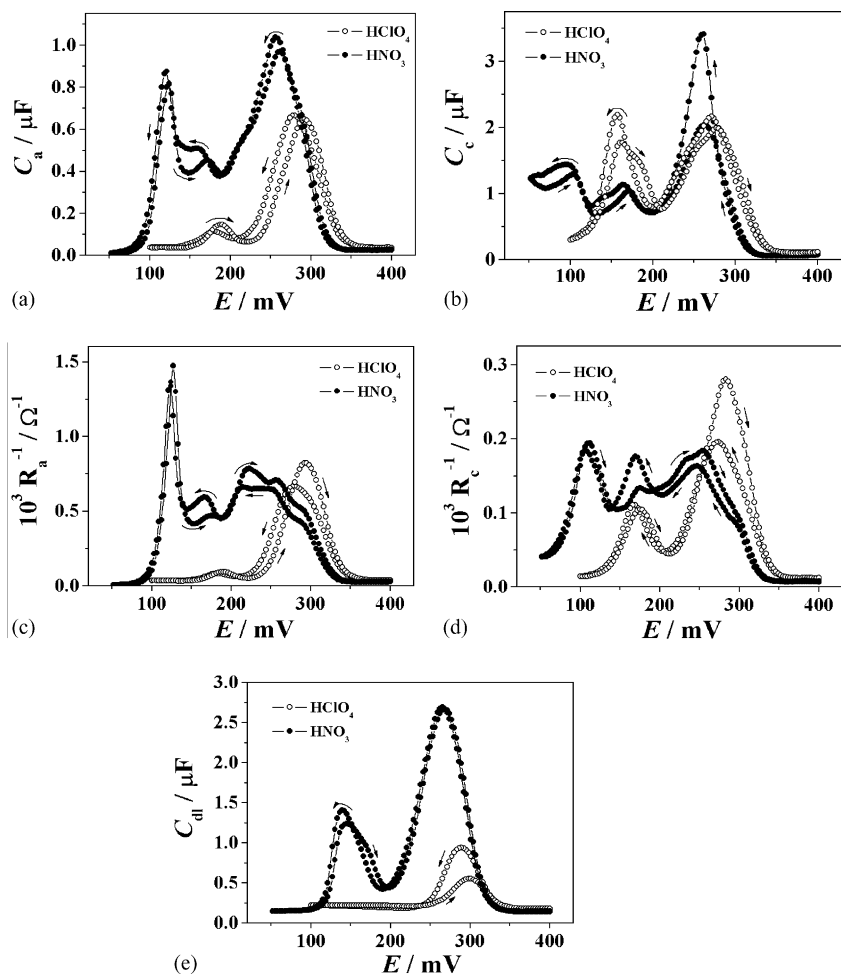


Fig. 10. EEC parameters of Bi upd on Au in nitric and perchloric solutions, as functions of the potential in cyclic scans. $dE/dt = 3.1$ mV/s.

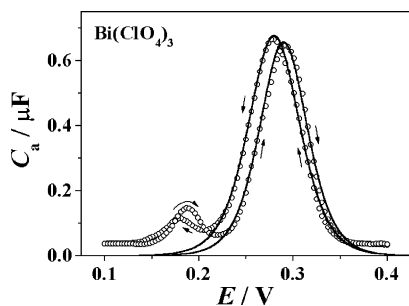


Fig. 11. Capacitance of perchlorate coadsorption in Bi upd on Au in cyclic scan; experimental data (open circles) and the curves simulated with Langmuir adsorption model (solid lines).

the formation and the destruction of the monolayer go by different paths, though locally the upd manifests reversible character.

Thus, in various features of the components of ac response Bi upd on Au shows hysteresis in cyclic potential scan and this hysteresis is probably due to the complexity of anions interaction with the monolayer manifested in characteristic dependences of EEC parameters on the potential.

5. PDEIS of aniline electropolymerisation

In stationary states of polymer films, dependences of EEC parameters on potential can be obtained by analysis of series of ac voltammograms with different modulation frequencies [30]. However, data from different scans cannot be juxtaposed in systems that alter in cycling. Electropolymerisation,

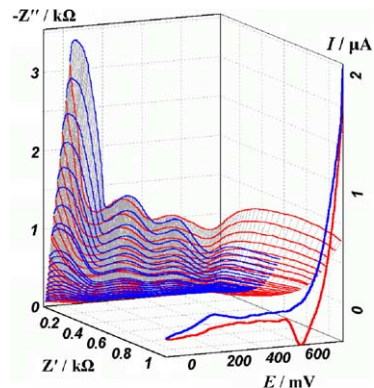


Fig. 12. PDEIS spectrum of aniline electropolymerisation on Au electrode.

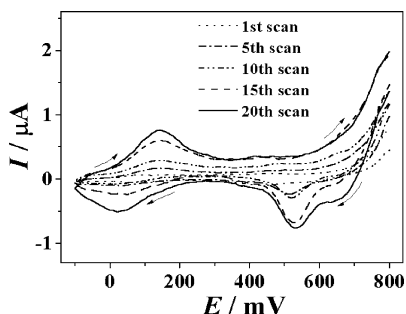


Fig. 13. CV of aniline electropolymerisation on Au electrode; $dE/dt = 27$ mV/s.

especially in initial stages, is a good example of the system strongly altered by cycling. Because of mobility of the electroactive polymer composition in electropolymerisation, CV is usually considered to be the best technique for both the monitoring and control of the electropolymerisation. PDEIS uses the same concept of the dynamic electrochemical response acquisition as the CV but, in addition to CV, gives more detailed information on the dynamics of electrostimulated transformations. The specific additional information comes from decomposition of ac response into constituents related to different EEC elements.

Fig. 12 shows a typical PDEIS spectrum of aniline electropolymerisation on Au electrode, Fig. 13 – cyclic voltammograms at various stages of continuous cycling during aniline electropolymerisation.

The analysis of PDEIS spectra of aniline electropolymerisation was applied without theoretical assumptions, using the automatic enumerative technique built into the program of the PDEIS spectrometer. The best-fit EEC obtained for initial four cycles is presented in Fig. 14. We would like to note again that the EEC in PDEIS is the model for decomposing the ac responses just in those frequencies that were tested. The circuit shown in Fig. 14 says nothing about possible specific responses in infralow, as well as in high frequencies. Nevertheless, this circuit has a reasonable physical meaning. Besides Faraday impedance, which appeared to be of diffusional origin (Warburg element in Fig. 14), and double layer capacitance C_{dl} , the EEC takes into account bulk properties of the growing polymer film represented by capacitance C_f and resistance R_f connected sequentially with the double layer capacitance.

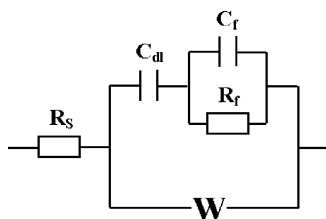


Fig. 14. EEC of aniline electropolymerisation on Au electrode (initial four scans).

Fig. 15 shows the variation of main parameters of the EEC in the four cyclic scans recorded sequentially with short stops in the end of each cycle at 800 mV. The animation to Fig. 12 appended to the electronic version of the manuscript gives the 3D view of the frequency response in different perspectives. Some specific features of ac response become apparent immediately from the spectrum. The ac response looks very differently in the ranges of redox transformations of polyaniline (approximately from -50 to 300 mV) and at higher potentials where the film grows (Fig. 12).¹ The processes at higher potential are more irreversible than at lower potential. Active component of impedance is very low at low potentials but increases considerably above 400 mV.

C_f and R_f^{-1} show a complex evolution in consecutive scans and increase considerably in first three scans (Fig. 15c and d). C_{dl} also increases fast with each scan but its signature on the potential scale is less variable than of C_f and R_f (Fig. 15a). The main increase in C_{dl} obviously results from the increase in the surface area of the conducting polymer formed in the reaction. The inverse of Warburg constant, A^{-1} shows small peaks in the forward and backward scans at potentials of polyaniline redox transformations, thus disclosing the presence of diffusion effects in the cathodic and anodic reactions in this range, but the main variation of A^{-1} falls on the active electropolymerisation range above 600 mV (Fig. 15b).

The variation of all parameters in Fig. 15 shows that the system under investigation changes rapidly during the cyclic testing. The small values of potential steps in the potential scan and the limitation in the frequency range in this case were especially important to secure measurements from drift effects. PDEIS spectrometer provided various means to control this in different levels of signal processing. For questionable cases, besides automatic control, the spectrometer has a waveform display to make sure that drift effects do not disturb measurements. Even for the lowest frequency, which was 12 Hz, the signals were undistorted at the scan rate of 1.6 mV/s in that experiment.

The goal of this example was just to show the possibility of PDEIS application for multi-parameter monitoring of nonstationary stages in electropolymerisation, so we will not speculate on the mechanisms of the processes that lie behind the complex variation of the parameters in Fig. 15. Even a cursory comparison of Figs. 13 and 15 gives the evidence of a vast domain of new information that becomes available when not only the dc response but also the frequency response is analysed in the same potential scan.

6. Summary

Potentiodynamic electrochemical impedance spectroscopy acquires, by means of a common potentiostat controlled with virtual instruments, multidimensional dependencies that

¹ Dynamic frequency response of polyaniline has been also investigated lately with a different kind of dynamic EIS by Darowicki and Kawula [31].

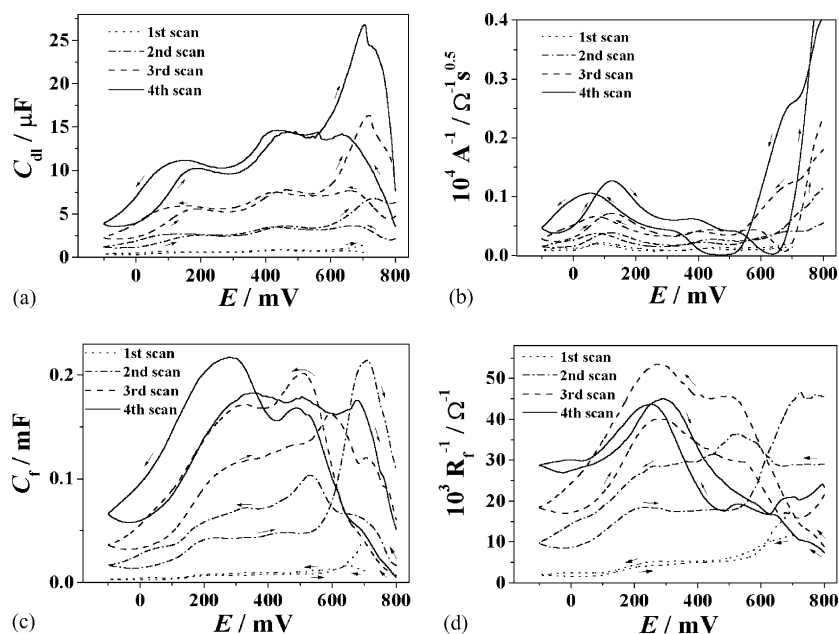


Fig. 15. EEC parameters of aniline electropolymerisation on Au electrode as function of the potential in initial four cyclic scans. $dE/dt = 1.6 \text{ mV/s}$.

characterise variations of dc current and frequency response in a potential scan. Unlike classical EIS, which investigates frequency response in stationary states in order to obtain the whole equivalent circuit, PDEIS acquires frequency response for a different purpose – it needs the information on frequency response in limited ranges of frequencies to decompose the ac response at certain frequencies into components belonging to different processes. For this purpose only those EEC elements are required, which contribute to the analysed response. Therefore, PDEIS uses narrow frequency ranges in its investigation of frequency response. Correspondingly, the main advancements in the probing and analysis implemented in PDEIS (application of wavelets, using very small potential steps in the potential scan in order to enable impedance analysis in three dimensions, digital elimination of 50 Hz noise) were aimed on better decomposition of the ac response. Due to the advancements in the potentiodynamic response probing, PDEIS enables individual monitoring of different processes in the potential scan.

The idea of PDEIS is very similar to the idea of dc and ac voltammetry. Similarly to a combination of the latter two techniques, PDEIS gives the information on the variation of dc and ac responses in a potential scan, but, unlike ac voltammetry, this new technique is equipped with means for presenting the potentiodynamic ac response as a set of constituent potentiodynamic responses of different elements of the EEC. The decomposition of the ac response extends the common potentiodynamic probing to new dimensions and enables fast multi-parameter characterisation of various systems, both reversible and irreversible.

Similarly to common dc voltammetry, which is helpful for characterisation of systems with different extent of irreversibility, from completely reversible to completely ir-

reversible, PDEIS also can analyse different systems. In this work PDEIS was applied to three kinds of systems, from completely reversible (ferricyanide redox transformations), through locally reversible but showing different paths for forward and backward scans (Bi up on Au), to completely irreversible (characterisation of initial stages of aniline electropolymerisation). In the first case the constituent potentiodynamic responses were compared with theoretical predictions and showed compliance with the theory. For the latter two systems there was no possibility to compare the experimental constituent responses with theoretical predictions, because in that part the investigation entered a yet unexplored domain of nonstationary systems potentiodynamic frequency response characterisation. We hope that the new experimental opportunities provided by PDEIS will stimulate the development of theory of constituent nonstationary potentiodynamic responses, and advances in theory will enable a transition from observation to explanation of complex irreversible potentiodynamic responses.

Appendix A. Supplementary data

Supplementary data associated with this article can be found, in the online version, at [doi:10.1016/j.electacta.2004.10.055](https://doi.org/10.1016/j.electacta.2004.10.055).

References

- [1] E. Yeager, A.J. Salkind, *Techniques of Electrochemistry*, Wiley, 1973.

- [2] R.A. Cottis, A.M. Llewellyn, *Electrochemical Techniques*, UMIST, 1996 (available from http://www.cp.umist.ac.uk/lecturenotes/Echem/index_main.htm).
- [3] C.B. Duke, E.W. Plummer (Eds.), *Frontiers in Surface and Interface Science*, Elsevier, Amsterdam, 2002.
- [4] S.C. Creason, D.E. Smith, J. *Electroanal. Chem.* 36 (1972) 257.
- [5] R.J. Schwall, A.M. Bond, R.J. Loyd, J.G. Larsen, D.E. Smith, *Anal. Chem.* 49 (1977) 1797.
- [6] R.J. Schwall, A.M. Bond, D.E. Smith, *Anal. Chem.* 49 (1977) 1805.
- [7] R.J. Schwall, A.M. Bond, D.E. Smith, J. *Electroanal. Chem.* 85 (1977) 217.
- [8] A.M. Bond, R.J. Schwall, D.E. Smith, J. *Electroanal. Chem.* 85 (1977) 231.
- [9] G.S. Popkirov, R.N. Schindler, *Rev. Sci. Instrum.* 63 (1992) 5366.
- [10] G.S. Popkirov, *Electrochim. Acta* 41 (1996) 1023.
- [11] J. Schiewe, J. Hazi, V.A. Vicente-Beckett, A.M. Bond, J. *Electroanal. Chem.* 451 (1998) 129.
- [12] M.J. Walters, J.E. Garland, C.M. Pettit, D.S. Zimmerman, D.R. Marr, D. Roy, J. *Electroanal. Chem.* 499 (2001) 48.
- [13] J.E. Garland, K.A. Assiongbon, C.M. Pettit, S.B. Emery, D. Roy, *Electrochim. Acta* 47 (2002) 4113.
- [14] J.G. Webster (Ed.), *Measurement, Instrumentation, and Sensors Handbook*, CRC Press, 1999.
- [15] G.A. Ragoisha, A.S. Bondarenko, *Solid State Phenom.* 90–91 (2003) 103 (free preprint is available from <http://www.sciencedirect.com/preprintarchive>).
- [16] G.A. Ragoisha, A.S. Bondarenko, *Electrochem. Commun.* 5 (2003) 392.
- [17] G.A. Ragoisha, A.S. Bondarenko, N.P. Osipovich, E.A. Streltsov, J. *Electroanal. Chem.* 565 (2004) 227.
- [18] G.A. Ragoisha, A.S. Bondarenko, *Surf. Sci.* 566–568 (2004) 315.
- [19] C.A. Schiller, F. Richter, E. Gülzow, N. Wagner, *Phys. Chem. Chem. Phys.* 3 (2001) 374.
- [20] P. Agarwal, O.D. Crisalle, M.E. Orazem, L.H. Garcia-Rubio, J. *Electrochem. Soc.* 142 (1995) 4149.
- [21] A. Lasia, in: B.E. Conway, J. Bockris, R. White (Eds.), *Modern Aspects of Electrochemistry*, vol. 32, Kluwer Academic/Plenum Publishers, New York, 1999, pp. 143–248.
- [22] A. Lasia, in: B.E. Conway, R. White (Eds.), *Modern Aspects of Electrochemistry*, vol. 35, 2002, pp. 1–49.
- [23] B.G. Dekker, M. Sluyters-Rehbach, J.H. Sluyters, J. *Electroanal. Chem.* 23 (1969) 9.
- [24] S. Morin, H. Dumont, B.E. Conway, J. *Electroanal. Chem.* 412 (1996) 39.
- [25] B.E. Conway, J. Barber, S. Morin, *Electrochim. Acta* 44 (1998) 1109.
- [26] G.A. Ragoisha, A.S. Bondarenko, *Chem. Problems Dev. New Mater. Technol., Minsk, BSU 1* (2003) 138 (free electronic preprint is available from <http://www.sciencedirect.com/preprintarchive>).
- [27] Z. Shi, S. Wu, J. Lipkowski, *Electrochim. Acta* 40 (1995) 9.
- [28] M.A. Schneeweiss, D.M. Kolb, *Phys. Status Solidi (a)* 173 (1999) 51.
- [29] E. Herrero, L.J. Buller, H.D. Abruna, *Chem. Rev.* 101 (2001) 1897.
- [30] O.A. Semenikhin, E.V. Ovsyannikova, N.M. Alpatova, Z.A. Rotenberg, J. *Electroanal. Chem.* 408 (1996) 67.
- [31] K. Darowicki, J. Kawula, *Electrochim. Acta* 49 (2004) 4829.